Open access • Journal Article • DOI:10.13031/2013.29140

Comparing methodologies for the characterization of water drops emitted by an irrigation sprinkler. — Source link

Carlos Bautista-Capetillo, R. Salvador, J. Burguete, J. Montero ...+4 more authors

Published on: 01 Jan 2009 - Transactions of the ASABE (American Society of Agricultural and Biological Engineers)

Topics: Impact sprinkler and Disdrometer

COMPARING METHODOLOGIES FOR THE CHARACTERIZATION OF WATER DROPS EMITTED BY AN IRRIGATION SPRINKLER

by

C. Bautista-Capetillo[1] *, R. Salvador[2], J. Burguete[2], J. Montero[3],

J. M. Tarjuelo[3], N. Zapata[2],J. González[1] and E. Playán[2]

Abstract

A variety of techniques have been proposed for sprinkler drop characterization. Two of them, the disdrometer method (D) and the low-speed photographic method (P), have recently been applied in the literature. A statistical method for the improvement of disdrometer measurements (DM) has been proposed to improve D measurements. The aims of this study were: 1) to compare the disdrometer and photographic methods under indoor conditions; 2) to produce a drop characterization data set; 3) to assess the effect of the statistical treatment of disdrometer data; and 4) to gain insight on the relationship between drop variables. The drops resulting from an impact sprinkler operating at 200, 300 and 400 kPa were characterized at distances of 3, 6, 9 and 12 m from the sprinkler. In each method, diameters responded to operating pressure and distance from the sprinkler according to the expected trends. The difference in volumetric diameter estimation between P and D amounted to -4% of the average P volumetric diameter. The application of DM to this data set increased the difference in volumetric diameter with method P to 15%. Drop velocity and angle could be measured with the P method, and showed clear relationships with drop diameter. Finally, regression equations were presented relating the most relevant experimental variables. The disdrometer resulted in fast measurements of drop diameter, while the

[1] Planeación de Recursos Hidráulicos, Universidad Autónoma de Zacatecas, 98000 Zacatecas, Mexico.

[2] Departamento Suelo y Agua., Estación Experimental de Aula Dei, CSIC. P. O. Box 13034, 50080 Zaragoza, Spain.

[3] E. T. S. I. Agrónomos, Universidad Castilla-La Mancha, Campus Universitario s/n 02071 Albacete, Spain.

* Corresponding author: baucap@uaz.edu.mx

photographic method provided additional variables but required intense work at the laboratory and particularly at the office.

Keywords: low-speed photography, disdrometer, drop diameter, velocity, angle, indoor, sprinkler irrigation.

Introduction

A sprinkler irrigation system distributes water as discrete drops traveling through the air. Drop characterization (variables such as diameter, velocity and trajectory) is required to design and evaluate a sprinkler irrigation system and to assess the relationship between the irrigation system, the soil and the crop. An adequate characterization of the drops emitted by a sprinkler irrigation system permits us to evaluate issues such as evaporation losses and kinetic energy. Sprinkler evaporation losses have been found to depend on the distribution of drop diameters. Under high vapor pressure deficit conditions, small drops are subjected to large evaporation losses (Thompson et al., 1993). However, when drop evaporation is controlled by air friction, large drops can account for most evaporation losses (Lorenzini and Wrachien, 2005). The kinetic energy with which drops impact on the soil is of particular concern when drop diameters are large (Kincaid et al., 1996). Finally, the frequency of different drop sizes has a significant effect on water distribution on the field and therefore on the uniformity of water application (Sudheer and Panda, 2000). Non-agricultural sprinkler applications, such as indoor fire protection, have based design and management procedures on relevant drop characterization efforts (Wu et al., 2007).

Drop diameter, velocity and trajectory from the nozzle to the soil surface depend on a number of factors. The most relevant are the type of sprinkler and nozzle, the operational hydraulic parameters and the environmental conditions at the particular location where the sprinkler system is or will be located. The ballistic theory constitutes the most common modeling approach to sprinkler irrigation, particularly with respect to solid-set systems (Fukui et al., 1980; Vories et al., 1987). Ballistic theory explains that the velocity of sprinkler drops approaching the soil surface is higher for large drops than for small drops. This is due to the effect of drop diameter on aerodynamic drag. An increase in sprinkler operating pressure results in smaller average drop diameter, and consequently in reduced average drop velocity. This discussion on drop diameter and velocity applies to calm wind conditions. In the presence of strong winds, the horizontal component of drop velocity may be more affected by the wind than by the initial drop velocity.

Despite recent analytical developments in sprinkler irrigation (De Wrachien and Lorenzini, 2006), a general ballistic model for impact sprinkler irrigation in the presence of wind is not currently available: existing models must be calibrated for

specific conditions. As a consequence, intense experimental work is required for the applicability of ballistic models for a particular combination of irrigation hardware and experimental conditions (Montero et al., 2001; Playán et al., 2006). This situation can be compared to that of surface irrigation. Numerical surface irrigation models can be calibrated using as little as one irrigation evaluation. The calibrated model can only be applied to the experimental soil conditions which, strictly speaking, only existed on the day of the experiment. Current ballistic sprinkler irrigation models require a number of experiments for their complete calibration. However, the calibrated model can be applied to a wide range of environmental conditions for the experimental irrigation hardware and operating conditions.

Different experimental methods to evaluate drop characteristics were reported in the literature during the 20th century and even before (Wiesner, 1895). Sudheer and Panda (2000) described a variety of techniques, proposed by different researchers, to determine sprinkler and rainfall drop diameter. According to these authors, the most common techniques include stain, photographic, flour pellet, momentum and oil-immersion. In a number of these methods photography was used to support diameter estimation. In some cases, digital image techniques have been introduced to accelerate data processing. In recent years, optical techniques, based on laser beams (Kincaid, 1996) or on the attenuation of a luminous flow - such as the disdrometer technique – (Montero et al., 2003) have been developed to evaluate sprinkler drop diameter.

An alternative procedure consists of using a ballistic model to simulate the landing distance of different drop diameters resulting from a given sprinkler and nozzle model, nozzle elevation, operating pressure and wind velocity (Fukui et al., 1980; Vories et al., 1987; Carrión et al., 2001; Playán et al., 2006). By this inverse procedure the drop diameter distribution reproducing the radial application pattern of a given sprinkler is identified. The resulting drop diameter data can be used to run scenario simulations using the ballistic model (Carrión et al., 2001; Playán et al., 2006). However, these data can only be compared with drop diameter measurements if the model uses an adequate representation of the physical processes involved. Since a number of concerns have been expressed in the literature about the underlying ballistic hypotheses (particularly in the presence of wind), data sets containing reliable measurements of drop diameter, velocity and trajectory are currently required to contribute to further model refinements.

This paper reports on the characterization of the drops emitted by an irrigation sprinkler in the absence of wind (indoor conditions). These variables were measured using two methods based on low-speed photography (Salvador et al., 2009) and on the use of a disdrometer (Montero et al., 2006; Burguete et al., 2007). The aims of this study were: 1) to compare different techniques of drop characterization in order to assess their reliability; 2) to produce and disseminate a drop characterization data set for further use in ballistic model refinements; 3) to assess the effects of the statistical treatment of disdrometer data; and 4) to gain insight on the relationship between variables such as drop diameter, velocity and angle.

Materials and Methods

Experimental procedure

The experiments were performed at the indoor facilities of the Irrigation Material Laboratory of the Department of Agriculture, Government of Castilla La Mancha, and University of Castilla La Mancha at Albacete, Spain. The experimental sprinkler was a VYR35 model (VYRSA, Burgos, Spain), equipped with a 4.8 mm nozzle. According to the catalogue, the sprinkler jet forms an angle of 26º with respect to the horizontal.

Determination of the radial sprinkler application pattern

In order to characterize the sprinkler, experiments were performed to determine the radial application pattern. The ISO 15886-3 norm (Anonymous, 2004) was followed in the design of the experimental set up and in the experiment itself. The pluviometers where cylindrical in shape, had a diameter of 0.16 m, and were spaced at 0.60 m intervals, to a distance of 18 m. The nozzle elevation over the top of the pluviometers was 0.50 m. Three experimental pressures were considered throughout this work: 200, 300 and 400 kPa. The radial application pattern from a rotating sprinkler was determined for each experimental pressure. The experiments had durations of 60, 58 and 61 min for pressures of 200, 300 and 400 kPa, respectively. Air and water temperature was 10ºC. Before performing the experiments, the sprinkler was run for a few minutes in order to standardize environmental conditions.

Drop characterization experiments

The experiment was designed to characterize drops at distances of 3, 6, 9 and 12 m from the sprinkler nozzle at the three experimental pressures (Fig. 1a). The experimental sprinkler was enclosed in a metal cylinder as described by Chen and Wallender (1985) and Tarjuelo et al. (1999), with a lateral slit that permitted to obtain a wedge shaped portion of the circular wetted area. Four observation points were arranged at the abovementioned distances. The nozzle was located 0.50 m above the drop characterization points. Drops emitted by the main jet and those created by the oscillations of the impact arm were analysed together at the distance of 3 m. At 6 m both groups of drops arrived separately at the observation point, and only drops emitted by the main jet were characterized. At further distances, only drops resulting from the main jet were present. At each observation point, drops were characterized

using two alternative methods: the photographic method (Salvador et al., 2009) and the optical disdrometer (Montero et al., 2006).

The photographic method for drop characterization proposed by Salvador et al. (2009) is based on low-speed photography of the drops emitted by the sprinkler (Fig. 1b). A reflex digital camera manufactured by Nikon (model D80) was used in this work. A screen was located at a distance of 0.80 m from the camera objective, and the camera was focused at a distance of 0.55 m, where a millimetric ruler attached to the screen was located to serve as an internal length reference. In low-speed photographs, drops were depicted as transparent cylinders (Fig. 1c). After a digital treatment of the photographs, drops were manually characterized by measuring the drop diameter (d, mm), the cylinder length (L) and the angle respect to the horizontal (θ, ^{o}). The drop angle was estimated in the vertical plane depicted by the photograph, and the 0^{o} angle was set in the horizontal direction from the drop to the sprinkler. An angle of 90^{o} represents a vertical falling drop. Angles below 90^{o} are expected in the experimental set-up. Drop velocity (V, m s^{-1}) was estimated from cylinder length and camera shutter speed (Fig. 1c). The indoor laboratory conditions required artificial lightning and modifications in the camera settings with respect to those optimised by Salvador et al. (2009). After a series of prospective experiments, we decided to locate a 200 W spotlight adjacent to the screen, illuminating it at 90^{o} angle. The camera was set at a diaphragm opening of F 5 and at a shutter speed of 100 (0.01 s). Photographs were taken in continuous mode (9 photos in the first 3.1 seconds, one photo each 1.13 seconds later on). A total of 1,263 photographs were taken at different distances and pressures, although only 413 contained valid drops. A total of 1,229 drops were characterized in these pictures. Only in-focus drops were considered valid for the purposes of this work. If only a portion of the drop was contained in the picture, its diameter and angle were recorded, but its velocity could not be estimated.

Salvador et al. (2009) performed a validation experiment of the photographic method. When drop measurements were compared to real diameters (using metal spheres) and simulated velocities (using the free fall equation), the resulting errors were -0.45 % for diameter (small underestimation), and 0.31 % for velocity (small overestimation). These authors concluded that the most relevant source of error was the fact that all drops passing at a distance of ±0.04 m from the target (marked with a dashed line in Fig. 1b) would appear as focused. Consequently, these drops would appear bigger or

smaller than they really are. Salvador et al. (2009) bounded this error as ±2.45 % for drop diameter and ±1.23 % for drop velocity. When analysing a set of drops, these errors compensate in the estimation of average diameters and velocities. However, the errors in the distribution of these variables may not compensate.

The office procedures for photographic drop characterization were very time consuming. Fig. 1c presents an example of the determinations performed for each drop. Salvador et al. (2009) reported a process time of 7 min drop^{-1}, a rate that also applied to this work. Consequently, 143 hours of office work were required to produce the resulting photographic drop data set.

An optical disdrometer model ODM 470, manufactured by Eigenbrodt (Königsmoor, Germany), was used for automatic drop characterization. The device is based on the attenuation of an infrared beam as drops pass through an optical window (Montero et al., 2006). The beam detector was circular in shape and had a diameter of 20 mm. The disdrometer performed continuous measurements as the drops emitted by the sprinkler fell. Each drop resulted in an attenuation of the signal. Signal analysis produced estimates of drop diameter and time of passage. The measurement principle of the disdrometer did not permit the measurement of drop angle. In the twelve experiments reported in this paper, the disdrometer characterized 13,254 drops. These drops constitute twelve sets of type D in the following analyses.

Montero et al. (2006) reported two experimental problems which affect the quality of disdrometer measurements. These problems are related to drop overlapping and drop passing through the side of the detector. In the first case, following the simultaneous passage of two drops, the detector will measure a larger-than-real drop. In the second case, a side-passing drop (partially detected by the device) will be measured as a smaller-than-real drop. Burguete et al. (2007) presented and validated a statistical procedure for the detection of these errors, based on the discrepancies between drop diameter and time of passage. This technique permits the identification of faulty drops which can be removed from the data set. For a given operational pressure and observation point, a disdrometer data set of size n was obtained. The average drop time of passage was obtained as:

$$\overline{T} = \frac{1}{n}\sum_{i=1}^{n} T_i \qquad [1]$$

where T_i is the time of passage for drop i and $\overline{T}$ is the average drop time of passage in the set. Geometric considerations on the detector radius R (10 mm in this case) and drop radius r_i led to the formulation of maximum and minimum times of passage for each drop (Burguete et al., 2007). Drop i is rejected if its T_i exceeds the maximum value or is lower than the minimum value:

$$T_i > (1+\tau)\frac{4}{\pi}\overline{T} \quad [2]$$

$$T_i < (1-\tau)\frac{8}{\pi}\frac{\sqrt{Rr_i}}{R+r_i}\overline{T} \quad [3]$$

The process is governed by a tolerance τ, and is formulated in an iterative way. The improved method for erroneous drop removal, described by Burguete et al. (2007) was used in this paper. This method automatically adjusts the value of τ. When the drop rejection procedure was applied to the twelve disdrometer data sets, the total number of drops was reduced to 6,530 (the average percentage of drop removal was 51%). The remaining drops in each set constitute the twelve sets of type DM in the following analyses.

The estimation of drop velocity (V) from disdrometer time of passage required specific considerations. Drops can pass through the central or lateral side of the detector. As a consequence, velocities should be obtained from the time of passage and the length of the drop trajectory projected on the detector. This trajectory ideally ranges between 0 and twice the detector radius, R. Burguete et al. (2007) derived a ratio of $\frac{\pi}{4}$ between the maximum and average drop times of passage. This ratio can be used to estimate velocity from drop time of passage:

$$V = \frac{\pi}{4}\frac{2R}{T_i} \quad [4]$$

Since the ratio is a statistical approximation, the proposed equation should be applied to a group of drops in order to determine their average velocity. As a consequence, drop velocity estimates derived from disdrometer data are presented in this paper for complete experimental data sets or for subsets corresponding to diameter ranges.

231 **Basic drop statistics: centrality and dispersion**

232 Managing the large data sets obtained from the photographic and disdrometer
233 methods required a statistical approach. While it is convenient to represent the sets by
234 a reduced number of parameters, some traits of the drop populations can be obscured
235 by the choice of statistical parameters. The parameters used in this work for drop
236 diameter included the arithmetic mean diameter (ϕ_A, mm), the volumetric mean
237 diameter (ϕ_V, mm) the volume median diameter (ϕ_{50}, mm), the standard deviation
238 (S_D, mm) and the coefficient of variation (CV_D, %). The volumetric mean, proposed by
239 Seginer (1963), was determined as:

240 $$\phi_V = \frac{\sum_{i=1}^{n} d_i^4}{\sum_{i=1}^{n} d_i^3} \quad [5]$$

241 Where d_i is the diameter of each drop in the set (mm), i is an ordinal extending from 1
242 to n, the number of drops in the set. Parameter ϕ_V corresponds to the volume weighted
243 average drop diameter. Parameter ϕ_{50} can be obtained by sorting all drops in the set by
244 diameter and selecting the drop diameter that represents 50% of the cumulative drop
245 volume.

246 The arithmetic mean, standard deviation and coefficient of variation were also used for
247 drop velocity (V_A and S_V, m s^{-1}; CV_V, %) and drop angle (θ_A and S_θ, °; CV_θ, %).

248

Results and Discussion

Radial application pattern

Figure 2 presents the radial application pattern for the experimental sprinkler setup operating at 200, 300 and 400 kPa. The maximum irrigation distance increased with pressure at an approximate rate of 0.01 m kPa^{-1}. The three radial curves showed a doughnut pattern which was previously described by several authors (Chen and Wallender, 1985; Li et al. 1994). The maximum value of precipitation rate was obtained at a distance of 0.60 m from the sprinkler for the three analyzed pressures (4.52 mm h^{-1} for 200 kPa; 5.20 mm h^{-1} for 300 kPa; and 5.93 mm h^{-1} for 400 kPa). Starting from this distance, the precipitation rate decreased to reach local minima. For 200 kPa, the minimum value was 1.06 mm h^{-1} at distances of 7.2 and 7.8 m from the sprinkler; for 300 and 400 kPa, local minimum values of precipitation rate of 1.56 mm h^{-1} and 1.68 mm h^{-1} were obtained at 3.6 m and 4.2 m from the sprinkler, respectively. At further distances precipitation rate increased to reach local maxima of 3.17 mm h^{-1} at 12 m for 200 kPa, 2.65 mm h^{-1} at 11.4 m for 300 kPa, and 2.72 mm h^{-1} between 10.2 and 11.4 m for 400 kPa.

Salvador et al. (2009) presented the radial application pattern for the same sprinkler and nozzle operating at 200 kPa under outdoor conditions. The outdoor pattern showed lower precipitation rate near the sprinkler (2.3 vs. 3.0 mm hr^{-1} at a distance of 1.5 m) and at the local maximum (2.75 mm hr^{-1} at 11 m outdoor vs. 3.17 mm hr^{-1} at 12 m indoor). These differences can be attributed to two factors: first, the vertical distance separating the sprinkler and the pluviometers was different in both cases, with 0.50 m in this work and 1.35 m in Salvador et al. (2009); and second, indoor experiments are subjected to very low evaporation losses, due to the complete absence of wind and to the humidification of the air before running the experiments. The maximum reach was larger for the indoor experiment (15.0 m vs. 14.4 m), although a larger reach would be expected outdoor because of the higher sprinkler elevation.

Drop characterization: basic statistics

Table 1 presents a number of statistical parameters for each combination of operating pressure and distance from the nozzle to the observation point. Results are presented for the photographic (P) method and the optical disdrometer method. In this last case, results are presented for the original data (D) and for the modifications introduced by

281 Burguete et al. (2007) (DM). As previously discussed, the drop angle could only be
282 measured by the photographic method. The complete data set, including individual
283 drop characteristics (P, D and DM) can be downloaded from www.eead.csic.es/drops.

284 For a given distance from the sprinkler, the mean drop diameter (arithmetic,
285 volumetric and median) usually decreased with an increase in operating pressure.
286 Between 200 and 400 kPa the volumetric drop diameter decreased by 4, 30, 34 and 43 %
287 (respect to the average values of P and D) for observation distances of 3, 6, 9 and 12 m,
288 respectively. The effect of pressure on drop diameter resulted more evident for large
289 distances to the sprinkler, as previously reported by Hills and Gu (1989). Additionally,
290 small drops concentrated in the vicinity of the sprinkler, leading to mean volumetric
291 and median diameters of about 1 mm, while volumetric and median diameters
292 exceeding 3 mm could be observed at a distance of 12 m for a pressure of 200 kPa.
293 Similar findings were previously reported by a number of authors. Recently Montero
294 et al. (2003) and Salvador et al. (2009) presented cumulative frequency charts and
295 histograms based on the disdrometer and the photographic method (respectively).
296 These frequency charts describe the distribution of drop diameters at each observation
297 point. Both authors reported a large variability of drop diameters, with average values
298 similar to those reported in this paper. In general, the standard deviation of drop
299 diameter increased with distance from the sprinkler and decreased with an increase in
300 operating pressure. The coefficients of diameter variation (determined from S_D and ϕ_A)
301 showed averages of 31.8, 44.0 and 36.3% for P, D and DM. In the case of P, no trend
302 could be detected for the coefficient of variation with distance or pressure. In the case
303 of D and DM the relationship of the coefficient of variation with distance from the
304 sprinkler was clear (from 19.1 to 67.6% for D and from 13.6 to 65.0% for DM, for
305 distances of 3 and 12 m, respectively).

306 Table 1 permits us to observe numerically the differences in the estimation of drop
307 diameter due to the selected method for drop characterization. Differences were small
308 in most cases, and relevant in some cases, with the previously discussed trends holding
309 for the photographic and disdrometer methods. A comparison was performed between
310 P on one hand and D and DM on the other, with the objective of assessing the effects of
311 the statistical method for drop rejection. The average differences (all pressures and
312 distances) in volumetric diameter between P and the disdrometer amounted to
313 -0.06 mm for D and 0.25 mm for DM. These differences represented -4% and 15% of the

314 average P volumetric diameter. The drop rejection method decreased the average
315 volumetric diameter by 0.31 mm. Consequently, the method rejected more volume of
316 large drops than of fine drops. When these differences were expressed in terms of
317 volume median diameter, the resulting values were 0.06 mm for P-D and 0.30 mm for
318 P-DM, corresponding to 4% and 18% of average P volume median diameter,
319 respectively.

320 Figure 3 presents a scatter plot of the photographic and disdrometer (D and DM) ϕ_V
321 measurements. Results are presented for the twelve combinations of distance from the
322 sprinkler and operating pressure. Regression lines are presented for D and DM, with
323 respective coefficients of determination of 0.900 and 0.941. The corresponding standard
324 errors were 0.258 and 0.202 mm. With a probability level of 0.95, the slope of both
325 regression lines was not statistically different from 1. Regarding the regression
326 intercept, the value for D was not statistically different from 0, while the value for DM
327 was. While DM explained a larger part of the variance in P than D did, variable D
328 could not be statistically distinguished from variable P (regression line with zero
329 intercept and unit slope). Both D and DM compared very well with P in terms of
330 volumetric diameter, but clear improvements could not be attributed in this
331 experiment to the statistical method for drop rejection.

332 Regarding drop velocity, relevant differences could be observed between the
333 photographic method on one side and the disdrometer and modified disdrometer on
334 the other (Table 1). Velocities were smaller when measured from photographs than
335 when estimated from disdrometer time of passage. The average difference between P
336 and D velocity estimates was -2.24 m s^{-1} (corresponding to 49% of average P velocity).
337 Regarding DM, the difference with P increased to -4.58 m s^{-1} (corresponding to 77% of
338 P velocity). Photographic velocity increased with distance and decreased with
339 operating pressure. The relationship between velocity and distance was previously
340 analyzed by Salvador et al. (2009) using the photographic method. These authors
341 reported velocities below 3 m s^{-1} for distances up to 3 m, and velocities of 4-6 m s^{-1} for
342 distances exceeding 10 m. The differences in velocity were attributed to differences in
343 drop diameter and consequently in aerodynamic drag.

344 When using velocity estimates from D or DM, a general trend in velocity could not be
345 deciphered with distance or pressure. This reflects the fact that the instrument was not
346 specifically designed to provide velocity estimates. As a consequence, the disdrometer

time of passage can be said to produce an approximation to average drop velocity. The standard deviation of P velocity increased with distance from the sprinkler. The average coefficient of P velocity variation was 16.5%, ranging from 11.0% at 3 m from the sprinkler to 18.3% at 12 m from the sprinkler. Although estimates of drop velocity are presented for D and DM, the standard deviation is not presented. This is due to the statistical approach used to estimate disdrometer drop velocity, which incorporates variability due to the length of the drop trajectory shadow on the detector. This variability cannot be differentiated from the variability in drop velocity.

The results for drop angle obtained with the P method were in agreement with the previous findings by Salvador et al. (2009) with respect to the relationship with distance. Our results confirm that at the largest distance (12 m), the angle and its variability decrease with respect to distances 3-9 m. The coefficient of variation did not show a clear trend with distance or pressure, and reached an average value of 8.1%. Small drops saw their trajectory more affected by air turbulences than larger drops. As a consequence, the conditions that favor small drops (small observation distances and high operating pressures) resulted in larger standard deviations. Small drops reached the observation points with a low horizontal velocity, and therefore showed large vertical angles, in the vicinity of 90^{o}. Large drops reached the observation points with a smaller horizontal angle, and showed a smaller standard deviation.

The results presented in Table 1 and Figure 3 led us to the conclusion that the DM procedure did not result in statistically better diameter measurements than the D procedure for the reported set of experimental values. Additionally, disdrometer velocity estimates were poor in all cases. As a consequence, the rest of the analyses in this paper were restricted to the P and D drop characterization methods for drop diameter, and to the P method for the characterization of drop velocity and angle.

Distribution of drop diameters

Drops landing at a certain distance cover a wide range of diameters. The range becomes wider as the distance from the sprinkler grows (Fig. 4). The disdrometer produced wider diameter ranges than the photographic method. Figure 4 further supports the idea that not all drops are formed at the nozzle (von Bernuth and Gilley, 1984; Seginer et al., 1991), since very small drops could be found at large distances from the sprinkler with the photographic and the disdrometer methods.

379 Figure 5 presents histographs of drop diameter for P and D, and for the twelve
380 combinations of pressure and distance from the sprinkler. The D method showed
381 presence of small drops (with diameter < 1 mm) at all four distances from the sprinkler
382 and in frequencies which usually exceeded 30%. The P method usually assigned lower
383 frequencies to small drops than the D method. As a consequence, drops exceeding
384 1 mm were more frequent in the photographic than in the disdrometer method. In an
385 extreme case, for a distance of 12 m and a pressure of 200 kPa, according to the
386 photographic method the smallest drops were 1.5 mm in diameter. Under the same
387 conditions, according to the D method, drops under 1 mm had a cumulative frequency
388 of 82.0%.

389 Figure 6 presents cumulative drop diameter frequencies as a function of drop diameter
390 for the different methodologies, distances and pressures. Figure 7 follows a similar
391 scheme, but for cumulative volume. When both Figures were compared, the slope of
392 the cumulative volume lines was less steep, indicating that this approach gives much
393 more relevance to larger drops, even if they appear at a very low frequency. Regarding
394 drop frequencies, the photographic method always showed more variability in drop
395 diameters than the disdrometer. This wider variability can be seen for a given pressure
396 and distance from the sprinkler (curves are less steep), but also among distances to the
397 sprinkler. When analyzing the methods in terms of cumulative volume, results are
398 more comparable, although large differences exist. In any case, at short distances from
399 the sprinkler, small drops were very significant for the D method. Additionally, small
400 drops accounted for about 10% of the volume at 12 m from the sprinkler in D (for all
401 pressures), while in the P method these drops had a negligible contribution to the
402 irrigation volume.

403 **Relationship between drop diameter, velocity and angle**

404 Figure 8 presents scatter plots of drop velocity *vs.* diameter for the photographic
405 method, and for the twelve combinations of pressure and distance. As previously
406 discussed, velocity estimates obtained from disdrometer time of passage (both D and
407 DM) only served the purpose of providing average drop velocity estimates. Plots in
408 Fig. 8 present individual drop data, and show a clear potential relationship between
409 diameter and velocity. The main difference between pressures is that at large pressures
410 drops larger than 3 mm are not present, and therefore the scatter plot shows drops
411 concentrated on the left side of the chart. The P method results in a relationship which

412 is readily comparable to the classical work of Laws (1941), cited by Cruvinel et al.
413 (1999). This agreement further supports the adequacy of photographic measurements
414 of drop velocity and diameter.

415 The results in Fig. 8 encouraged us to develop a diameter-velocity relationship for
416 individual drops (pooling all pressures and distances to the sprinkler). The resulting
417 scatter plot is presented in Fig. 9. The validity of a regression equation on these data
418 would be restricted to the experimental range in drop diameters and pressures, and
419 particularly to the difference in elevation between the sprinkler and the camera
420 (0.50 m). In order to address this limitation, a new data series was added to Figure 9,
421 corresponding to the experiments by Salvador et al. (2009). The latter data set was
422 obtained in outdoor conditions and with a difference in elevation sprinkler-camera of
423 1.35 m. A logarithmic regression equation was obtained for the combination of both
424 data series:

425 $$V = 2.28\, ln(d) + 3.25 \qquad [11]$$

426 with a coefficient of determination of 0.885 (probability level 0.999). The statistical
427 strength of the resulting model suggests that in the experimental range of conditions
428 drops reach a terminal velocity, independent of the difference in elevation between the
429 sprinkler and the camera. As a consequence, Eq. [11] is proposed to estimate individual
430 drop velocity from drop diameter (with a standard error of 0.431 m s^{-1}). This equation
431 could be applied to revise the statistical method for drop rejection proposed by
432 Burguete et al. (2007).

433 Regarding drop angle, results were only available for the P method (Fig. 10). Scatter
434 plots are presented for each distance from the sprinkler, and include a dashed line
435 located at an angle of 90^{o}, which the drops should not exceed given the relative
436 position of the sprinkler and the camera. Although a number of research works have
437 been devoted to drop characterization under sprinkler irrigation, the work by Salvador
438 et al. (2009) is the only known precedent to the analysis of drop angle. As previously
439 discussed, these authors researched on the same sprinkler, nozzle and a pressure of
440 200 kPa. The most relevant difference between both experiments is the vertical distance
441 between the sprinkler and the camera (1.35 m in the reference and 0.50 m in this work).
442 This difference anticipates smaller angles in this work than in Salvador et al. (2009). For
443 each experimental pressure, Figure 10 shows a decrease in the average drop angle with
444 the distance from the sprinkler. A large amplitude in drop angle could be appreciated

445 for small drops (<1 mm), apparently due to the erratic drop trajectory of these very fine
446 drops. Salvador et al. (2009) identified this trait in their outdoor experiment.
447 Considering the same distances to the sprinkler analyzed in this work, and referring to
448 the 200 kPa pressure, Salvador et al (2009) reported that drop angle fluctuated in the
449 range 40-90º for drops under 1 mm in diameter. In the indoor experiments reported in
450 this article (excluding two drops at the distance of 3 m), the range in drop angle was
451 65-95º. The amplitude of the range was therefore reduced from 50º outdoor to 30º
452 indoor. Figure 10 shows interesting differences between the experimental pressures,
453 particularly at the distance of 12 m. For median and large drops the drop angle clearly
454 increased with pressure, indicating a more vertical trajectory (by about 10º for 2 mm
455 drops in the pressure range of 200-400 kPa).

456 **Prediction of drop diameter, velocity and angle**

457 The encouraging results obtained for the disdrometer method (drop diameter) and the
458 photographic method (drop diameter, velocity and angle) led us to the development of
459 predictive equations oriented to practical irrigation system design and management
460 applications (Table 2). These included the estimation of volumetric mean diameter (ϕ_V)
461 and volume median diameter (ϕ_{50}) from distance from the sprinkler (x), and the
462 estimation of drop velocity and angle from ϕ_V and ϕ_{50}. Exponential, logarithmic, and
463 linear regression equations were proposed in Table 2 for different pressures and for the
464 average pressure. The coefficients of determination ranged from 0.730 and 0.999. These
465 equations can be considered representative of indoor, windless operation of the
466 specified sprinkler and nozzle model at 0.50 m elevation over the soil surface.

467

Summary and conclusions

This paper presents the comparison of two drop characterization methods: the photographic method (P) and the disdrometer method (D and DM). The P method sampled a relatively small number of drops (1,229). The original disdrometer method (D) measured all drops passing through the device in a given time (13,254 drops in the experimental conditions). Finally, the modified disdrometer procedure resulted in a reduced data set (6,530 drops). Increasing the number of drops in the set would require virtually no effort in the case of D and DM, while in the case of method P, drop characterization is particularly costly in terms of processing time.

The photographic and disdrometer methods produced diameter estimations responding to operating pressure and distance from the sprinkler according to the expected trends. The average drop diameters (ϕ_V) were 1.67 mm for P, 1.74 for D and 1.42 mm for DM. The average differences in volumetric diameter between P and the disdrometer amounted to -0.06 mm for D and 0.25 mm for DM (corresponding to -4% and 15% of the average photographic volumetric diameter). The arithmetic mean, volumetric mean and volume median diameters determined at different distances from the sprinkler were generally smaller for DM than for D (0.31 mm for ϕ_V on the average of all pressures and distances). While DM volumetric diameter explained a larger part of the variance in P volumetric diameter than D, a regression analysis indicated that D could not be statistically distinguished from P in terms of volumetric diameter. In the experimental conditions, the DM data set did not show a clear advantage in comparison with D data.

Regarding drop velocity, the quality of P measurements was endorsed by their relationship with drop diameter. P velocities ranged between 2.43 and 6.06 m s^{-1}, and averaged 3.66 m s^{-1}. The estimation of disdrometer drop velocity from time of passage was attempted, but produced poor results, even for average values. Finally, drop angle was only measured by the P method, constituting an added value of this methodology. Although the angle is not a central variable in drop characterization, it could be used to address a number of pending issues in ballistic model formulation. The average drop angle was 79.5º, ranging between an average of 81.6º at a distance of 3 m, and an average of 70.1º at a distance of 12 m.

499 Regression equations were presented for the estimation of drop volumetric mean
500 diameter and volume median diameter from distance from the sprinkler (using P and
501 D), and for the estimation of drop velocity and drop angle from volumetric mean
502 diameter and volume median diameter (using P data). These relationships explained
503 relevant percentages of data variance (73.0 - 99.9%), and can be used to characterize
504 mean values of the dependent variables under the experimental conditions.

505 Methods P and D produced drop diameter estimates that showed reasonable
506 agreement. The P method additionally produced measurements of drop velocity and
507 angle, which showed adequate relationships with other drop variables. The
508 photographic method provided valuable additional information as compared to the
509 disdrometer. However, this method is currently very labor intensive at the office. As a
510 consequence, the method will not be used in a routine fashion unless image processing
511 is automated. Data sets such as the one presented in this work are required for
512 methodology comparison and ballistic analyses. The disdrometer stands as a fast
513 method to characterize drop diameter. The drop rejection methodology introduced by
514 Burguete et al. (2007) did not show clear improvements over method D in this
515 particular case. However, the comprehensive data set presented in this work contains
516 valuable information for its refinement. For instance, the logarithmic regression
517 equation relating drop diameter and velocity, obtained from two independent
518 photographic data sets, could be used as an additional criterion to guide the drop
519 rejection process.

520

Acknowledgements

This research was funded by the Plan Nacional de I+D+i of the Government of Spain, through grant AGL2007-66716-C03. Carlos Bautista-Capetillo received a scholarship from the Agencia Española de Cooperación Internacional para el Desarrollo (AECID). Thanks are also due to the Universidad Autónoma de Zacatecas, México. The order of authors in the paper follows the "first-last-author-emphasis" criterion.

References

Anonymous. 2004. Agricultural irrigation equipment - Sprinklers Part 3: Characterization of distribution and test methods. ISO 15886-3/2004. International Organization for Standardization. Geneva, Switzerland. 15 pp.

Burguete, J., E. Playán, J. Montero, and N. Zapata. 2007. Improving drop size and velocity estimates of an optical disdrometer: Implications for sprinkler irrigation simulation. *Transactions of the ASABE* 50(6): 2103-2116.

Carrión, P., J. M. Tarjuelo, and J. Montero. 2001. SIRIAS: a simulation model for sprinkler irrigation. I Description of model. *Irrigation Science* 20: 73-84.

Chen, D. D., and W. W. Wallender. 1985. Droplet size distribution and water application with low-pressure sprinklers. *Transactions of the ASAE* 28(2): 511-516.

Cruvinel, P. E., S. R. Vieira, S. Crestana, E. R. Minatel, M. L. Mucheroni, and A. T. Neto. 1999. Image processing in automated measurements of raindrop size and distribution. *Computers and Electronics in Agriculture* 23(1999): 205-217.

De Wrachien, D., and G. Lorenzini. 2006. Modelling jet flow and losses in sprinkler irrigation: Overview and perspective of a new approach. Biosystems engineering, 94(2), 297-309.

Fukui, Y., K. Nakanishi, and S. Okamura. 1980. Computer evaluation of sprinkler irrigation uniformity. *Irrigation Science* 2: 23-32.

Hills, D. J., and Y. Gu. 1989. Sprinkler volume mean droplet diameter as a function of pressure. *Transactions of the ASAE* 32(2): 471-476.

Kincaid D. C. 1996. Spraydrop kinetic energy from irrigation sprinklers. *Transactions of the ASAE* 39(3):847-853.

Kincaid, D. C., K. H. Solomon, and J. C. Oliphant. 1996. Drop size distributions for irrigation sprinklers. *Transactions of the ASAE* 39(3): 839-845.

Li, J., H. Kawano, and K. Yu. 1994. Droplet size distributions from different shaped sprinklers nozzles. *Transactions of the ASAE* 37(6): 1871-1878.

Lorenzini, G., and D. De Wrachien. 2005. Performance assessment of sprinkler irrigation systems: A new indicator for spray evaporation losses. Irrigation and Drainage, 54(3), 295-305.

558 Montero, J., J. M. Tarjuelo, and P. Carrión. 2001. SIRIAS: a simulation model for
559 sprinkler irrigation. II Calibration and validation of the model. *Irrigation Science* 20:
560 85-98.

561 Montero, J., J. M. Tarjuelo, and P. Carrión. 2003. Sprinkler droplet size distribution
562 measured with an optical spectropluviometer. *Irrigation Science* 22: 47-56.

563 Montero, J., P. Carrión, J. M. Tarjuelo, and R. Nin. 2006. Calibración de un Disdrómetro
564 óptico para la medida de los tamaños de gota producidas por los aspersores. *XXIV*
565 *Congreso Nacional de Riego,* Lugo, Spain p. 148-149.

566 Playán, E., N. Zapata, J. M. Faci, D. Tolosa, J. L. Lacueva, J. Pelegrín, R. Salvador,
567 I. Sánchez, and A. Lafita. 2006. Assessing sprinkler irrigation uniformity using a
568 ballistic simulation model. *Agricultural Water Management* 84: 86-100.

569 Salvador, R., C. Bautista-Capetillo, J. Burguete, N. Zapata and E. Playán. 2009. A
570 photographic methodology for drop characterization in agricultural sprinklers.
571 *Irrig. Sci.* 27(4), 307-317.

572 Seginer, I. 1963. Water distribution from median pressure sprinkler. *J. Irrigation and*
573 *Drainage Division, ASCE* 89(IR2):13-29.

574 Seginer, I., D. Nir, and R. D. von Bernuth. 1991. Simulation of wind-distorted sprinkler
575 patterns. *J. Irrigation and Drainage Division, ASCE* 117(2): 285-306.

576 Sudheer, K. P., and R. K. Panda. 2000. Digital image processing for determining drop
577 sizes from irrigation spray nozzles. *Agricultural Water Management* 45 (2000) 159-
578 167.

579 Tarjuelo, J. M., J. Montero, M. Valiente, F. T. Honrubia, and J. Ortiz. 1999. Irrigation
580 uniformity with median size sprinklers. Part I. Characterization of water
581 distribution in no-wind conditions. *Transactions of the ASAE* 42(3): 665-675.

582 Thompson, A. L., J. R. Gilley and J. M. Norman. 1993. A sprinkler water droplet
583 evaporation and plant canopy model. 2. Model application. Transactions of the
584 ASAE 36(3): 743-750.

585 Vories, E. D., R. D. von Bernuth, and R. H. Mickelson. 1987. Simulating sprinkler
586 performance in wind. *J. Irrigation and Drainage Division, ASCE* 113(1): 119-130.

587 von Bernuth, R. D., and J. R. Gilley. 1984. Sprinkler droplet size distribution estimation
588 from single leg test data. *Transactions of the ASAE* 27(5): 1435-1441.

589 Wiesner, J. 1895. Beiträge zur Kentniss der Grösze des tropischen Regens. Akademie
590 der Wissenschaften, Mathematika-Naturwissenschaften Klasse, vol. 104, Sitz Berlin
591 Verlag, pp 1397–1434.

592 Wu, D., D. Guillemin, and A. W. Marshall. 2007. A modeling basis for predicting the
593 initial sprinkler spray. *Fire Safety Journal, ELSEVIER* 42(2007) 283-294.

594

595 # List of Tables

596 **Table 1.** *Statistical parameters for drop diameter, velocity and angle obtained for combinations*
597 *of operating pressure and distance from the sprinkler. Parameters include the arithmetic mean,*
598 *standard deviation and coefficient of variation (for diameter, velocity and angle), the volumetric*
599 *mean and the volume median diameter. Results are presented for methods P, D and DM.*

600 **Table 2.** *Predictive equations for the estimation of volumetric mean diameter (ϕ_v) and volume*
601 *median diameter (ϕ_{50}) from distance from the sprinkler (x), and for the estimation of drop*
602 *velocity (V) and drop angle (θ) from volumetric mean diameter and volume median diameter.*
603 *Regressions were obtained from the P and D data sets as indicated. The value of R^2 follows each*
604 *regression equation.*

605

606 # List of Figures

607 **Figure 1.** *Experimental set-up, detailing the location of the drop characterization points, the*
608 *arrangement of the camera, the screen and the spot light, and displaying a typical drop*
609 *photograph.*

610 **Figure 2.** *Radial application pattern for the experimental sprinkler setup operating at 200, 300*
611 *and 400 kPa.*

612 **Figure 3.** *Scatter plot of P volumetric diameter vs. D and DM volumetric diameters for all*
613 *pressures and distances to the sprinkler. Regression lines, equations, coefficients of*
614 *determination (R^2) and standard errors (SE) are presented for both dependent variables.*

615 **Figure 4.** *Drop diameters at distances of 3, 6, 9 and 12 m from the sprinkler for the drop*
616 *characterization methods P and D and the three operating pressures (200, 300 and 400 kPa).*

617 **Figure 5.** *Histographs of drop diameter for the P and D drop characterization methods and the*
618 *three operating pressures.*

619 **Figure 6.** *Curves of cumulative drop frequency at 3, 6, 9 and 12 m from the sprinkler for the P*
620 *and D drop characterization methods and the three operating pressures.*

621 **Figure 7.** *Curves of cumulative application volume at 3, 6, 9 and 12 m from the sprinkler for*
622 *the P and D drop characterization methods and the three operating pressures.*

623 **Figure 8.** *Relationship between drop diameter and drop velocity for the photographic method*
624 *(P), the four distances to the sprinkler and the three operating pressures.*

625 **Figure 9.** *Relationship between drop diameter and drop velocity obtained with the photographic*
626 *method (P). Data are presented corresponding to the results of Salvador et al. (2009) (using a*
627 *pressure of 200 kPa and different distances to the sprinkler) and to all the experimental results*
628 *reported in this paper (using different pressures and distances to the sprinkler). The logarithmic*
629 *regression, coefficient of determination (R^2) and standard error (SE) were obtained pooling both*
630 *data series.*

631 **Figure 10.** *Relationship between drop diameter and drop angle for the photographic method (P).*
632 *Results are presented for the four observation distances and the three operating pressures. The*
633 *dashed line represents an angle of 90° (vertical drop trajectory).*

Table 1. *Statistical parameters for drop diameter, velocity and angle obtained for combinations of operating pressure and distance from the sprinkler. Parameters include the arithmetic mean, standard deviation and coefficient of variation (for diameter, velocity and angle), the volumetric mean and the volume median diameter. Results are presented for methods P, D and DM.*

			P				D				DM			
			Distance from the Sprinkler (m)				Distance from the Sprinkler (m)				Distance from the Sprinkler (m)			
Operating Pressure (kPa)	Variable		3	6	9	12	3	6	9	12	3	6	9	12
200	Diameter (mm)	ϕ_A	0.86	1.04	1.50	3.08	0.89	0.98	1.19	1.05	0.81	0.78	1.02	0.97
		ϕ_V	1.12	1.48	1.93	3.28	1.02	1.96	2.29	3.36	0.87	1.10	1.76	3.36
		ϕ_{50}	1.05	1.40	1.92	3.59	0.89	1.83	1.97	3.71	0.79	0.80	1.70	3.68
		S_D	0.26	0.37	0.49	0.88	0.17	0.44	0.53	0.71	0.11	0.20	0.42	0.63
		CV_D	30.2	35.6	32.7	28.6	19.1	44.9	44.5	67.6	13.6	25.6	41.6	65.0
	Velocity (m s^{-1})	V_A	2.72	3.06	4.19	6.06	5.67	6.22	5.38	6.45	8.75	9.33	7.88	8.17
		S_V	0.34	0.64	0.75	1.04	-	-	-	-	-	-	-	-
		CV_V	12.5	20.9	17.9	17.2	-	-	-	-	-	-	-	-
	Angle (º)	θ_A	77.8	84.8	75.6	60.0	-	-	-	-	-	-	-	-
		S_θ	7.91	7.00	8.62	3.75	-	-	-	-	-	-	-	-
		CV_θ	10.2	8.26	11.4	6.25	-	-	-	-	-	-	-	-
300	Diameter (mm)	ϕ_A	0.81	1.03	1.22	2.06	0.84	0.87	1.08	1.34	0.78	0.76	0.90	1.21
		ϕ_V	1.08	1.43	1.44	2.65	0.94	1.32	1.86	2.74	0.82	0.87	1.42	2.32
		ϕ_{50}	1.06	1.40	1.39	2.55	0.82	0.98	1.56	2.51	0.76	0.75	1.24	2.35
		S_D	0.26	0.38	0.30	0.61	0.14	0.26	0.42	0.76	0.09	0.14	0.31	0.68
		CV_D	32.1	37.0	24.6	29.6	16.7	29.9	38.9	56.7	11.5	18.4	34.4	56.2
	Velocity (m s^{-1})	V_A	2.45	2.92	3.82	5.13	6.65	6.35	5.50	5.51	9.39	9.32	8.27	6.03
		S_V	0.19	0.61	0.59	1.00	-	-	-	-	-	-	-	-
		CV_V	7.76	20.89	15.45	19.49	-	-	-	-	-	-	-	-
	Angle (º)	θ_A	83.4	87.0	81.1	71.2	-	-	-	-	-	-	-	-
		S_θ	6.31	5.46	7.51	5.85	-	-	-	-	-	-	-	-
		CV_θ	7.57	6.28	9.26	8.21	-	-	-	-	-	-	-	-
400	Diameter (mm)	ϕ_A	0.86	0.96	1.19	1.45	0.81	0.86	0.97	1.30	0.77	0.76	0.79	1.22
		ϕ_V	1.19	1.25	1.46	1.78	0.87	1.16	1.33	2.00	0.80	0.87	0.99	1.91
		ϕ_{50}	1.17	1.18	1.42	1.73	0.78	0.93	1.21	1.94	0.74	0.75	0.79	1.87
		S_D	0.30	0.30	0.34	0.40	0.12	0.23	0.31	0.56	0.09	0.13	0.18	0.52
		CV_D	34.9	31.3	28.6	27.6	14.8	26.7	32.0	43.1	11.7	17.1	22.8	42.6
	Velocity (m s^{-1})	V_A	2.43	2.96	3.72	4.42	6.90	5.90	5.52	4.73	9.15	8.54	8.91	5.12
		S_V	0.31	0.51	0.66	0.80	-	-	-	-	-	-	-	-
		CV_V	12.8	17.2	17.7	18.1	-	-	-	-	-	-	-	-
	Angle (º)	θ_A	83.6	87.0	83.4	79.1	-	-	-	-	-	-	-	-
		S_θ	7.19	5.56	6.50	5.28	-	-	-	-	-	-	-	-
		CV_θ	8.60	6.39	7.80	6.68	-	-	-	-	-	-	-	-

638 **Table 2.** *Predictive equations for the estimation of volumetric mean diameter (ϕ_v) and volume median diameter (ϕ_{50}) from distance from the sprinkler (x), and*
639 *for the estimation of drop velocity (V) and drop angle (θ) from volumetric mean diameter and volume median diameter. Regressions were obtained from the P and*
640 *D data sets as indicated. The value of R^2 follows each regression equation.*

641

		Operating pressure (kPa)			
Drop Characteristics	Method	200	300	400	All
Diameter (mm)	P	$Ø_V=0.752\ e^{0.116x}$ ($R^2=0.969$)	$Ø_V=0.794\ e^{0.090x}$ ($R^2=0.848$)	$Ø_V=0.997\ e^{0.045x}$ ($R^2=0.942$)	$Ø_V=6.462\ P^{-0.36}\ e^{0.084x}$ ($R^2=0.839$)
		$Ø_{50}=0.656\ e^{0.133x}$ ($R^2=0.961$)	$Ø_{50}=0.785\ e^{0.088x}$ ($R^2=0.836$)	$Ø_{50}=0.967\ e^{0.045x}$ ($R^2=0.901$)	$Ø_{50}=7.441\ P^{-0.40}\ e^{0.089x}$ ($R^2=0.810$)
	D	$Ø_V=0.779\ e^{0.124x}$ ($R^2=0.939$)	$Ø_V=0.652\ e^{0.118x}$ ($R^2=0.999$)	$Ø_V=0.662\ e^{0.087x}$ ($R^2=0.965$)	$Ø_V=23.903\ P^{-0.62}\ e^{0.110x}$ ($R^2=0.955$)
		$Ø_{50}=0.625\ e^{0.145x}$ ($R^2=0.927$)	$Ø_{50}=0.511\ e^{0.127x}$ ($R^2=0.965$)	$Ø_{50}=0.542\ e^{0.099x}$ ($R^2=0.948$)	$Ø_{50}=31.094\ P^{-0.71}\ e^{0.124x}$ ($R^2=0.934$)
Velocity (m s^{-1})	P	$V=3.247\ Ln(Ø_V)+2.098$ ($R^2=0.974$)	$V=2.965\ Ln(Ø_V)+2.264$ ($R^2=0.906$)	$V=4.722\ Ln(Ø_V)+1.786$ ($R^2=0.966$)	$V=3.196\ Ln(Ø_V)+2.197$ ($R^2=0.931$)
		$V=2.830\ Ln(Ø_{50})+2.368$ ($R^2=0.982$)	$V=3.012\ Ln(Ø_{50})+2.329$ ($R^2=0.896$)	$V=4.559\ Ln(Ø_{50})+1.990$ ($R^2=0.936$)	$V=2.945\ Ln(Ø_{50})+2.380$ ($R^2=0.925$)
Angle (°)	P	$\theta=94.12-10.02Ø_V$ ($R^2=0.823$)	$\theta=95.18-8.972Ø_V$ ($R^2=0.802$)	$\theta=98.05-10.410Ø_V$ ($R^2=0.730$)	$\theta=96.98-10.440Ø_V$ ($R^2=0.812$)
		$\theta=91.54-8.534Ø_{50}$ ($R^2=0.846$)	$\theta=95.42-9.218Ø_{50}$ ($R^2=0.795$)	$\theta=98.33-10.960Ø_{50}$ ($R^2=0.791$)	$\theta=95.22-9.501Ø_{50}$ ($R^2=0.835$)

642

643

644 **Figure 1.** *Experimental set-up, detailing the location of the drop characterization points, the arrangement of the camera, the screen and the spot light, and*
645 *displaying a typical drop photograph.*

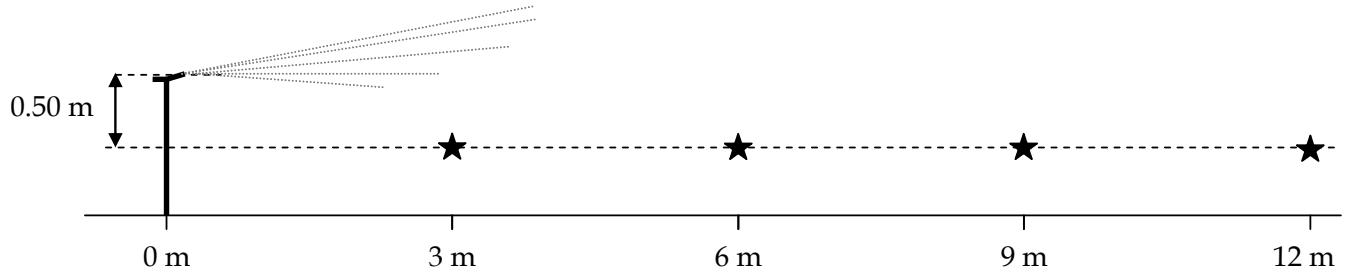

a) Experimental set-up for sprinkler characterization

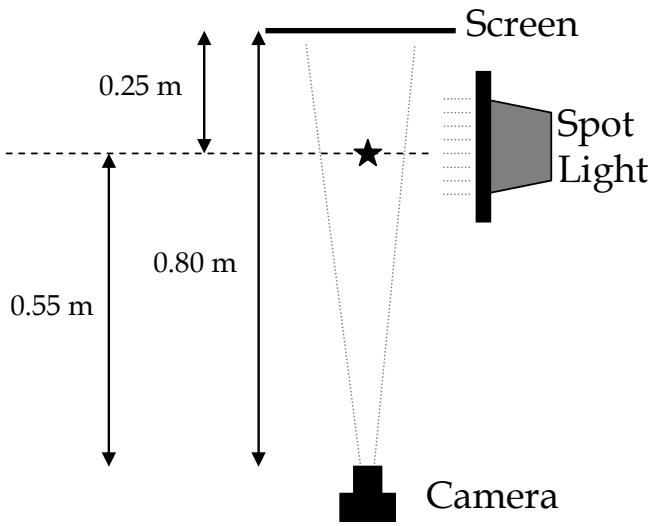

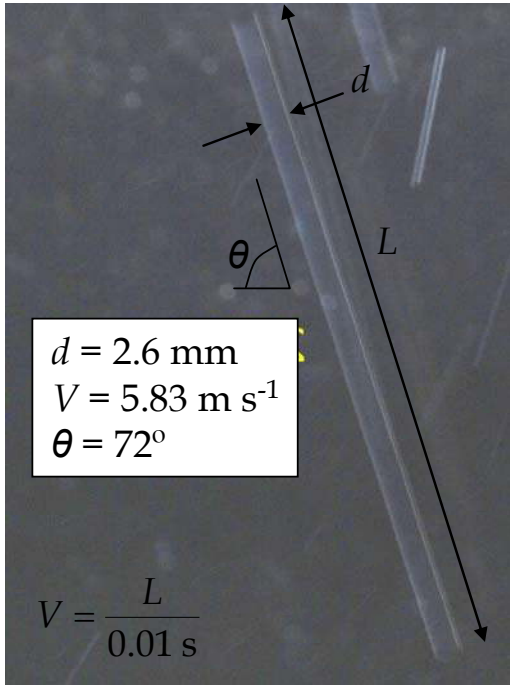

b) Plan view of the drop photography area **c) Typical drop photograph**

★) Drop characterization points

646

647

Figure 2. *Radial application pattern for the experimental sprinkler setup operating at 200, 300 and 400 kPa.*

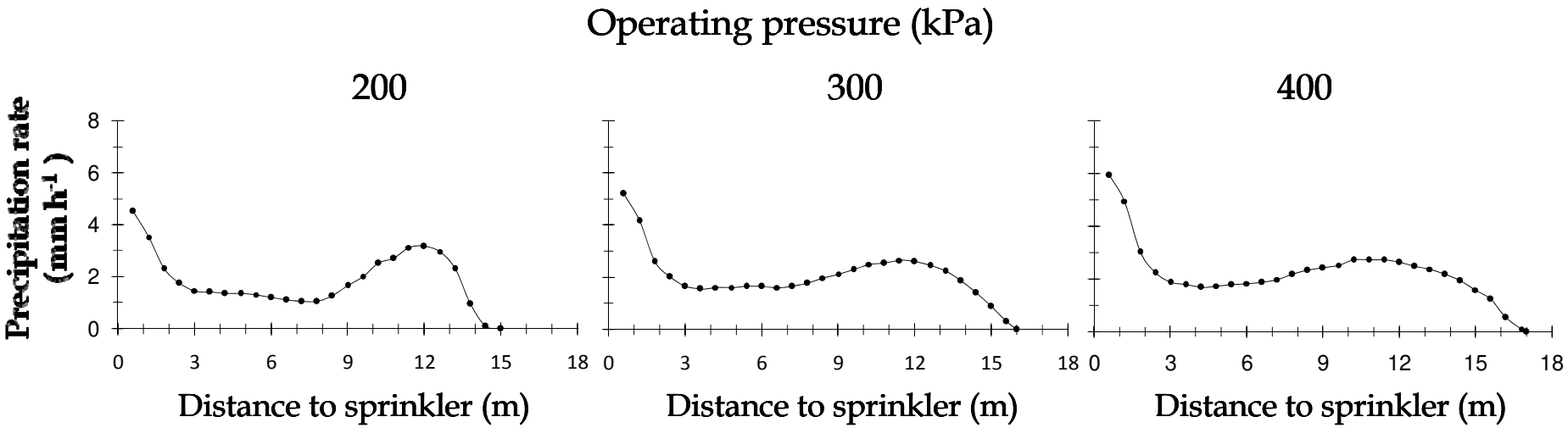

652 **Figure 3.** *Scatter plot of P volumetric diameter vs. D and DM volumetric diameters for all pressures and distances to the sprinkler. Regression lines, equations,*
653 *coefficients of determination (R^2) and standard errors (SE) are presented for both dependent variables.*

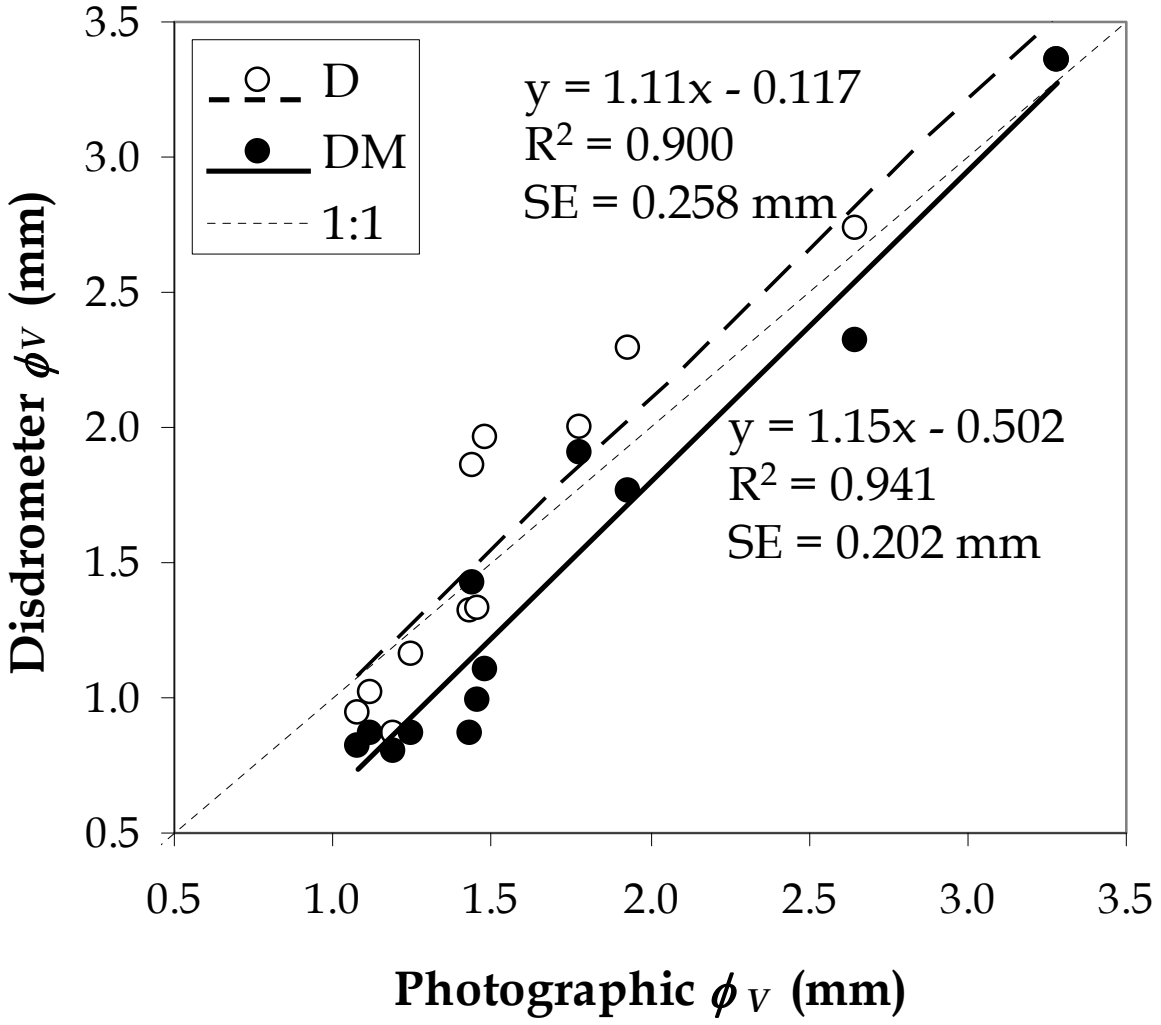

654

655

656 **Figure 4.** *Drop diameters at distances of 3, 6, 9 and 12 m from the sprinkler for the drop characterization methods P and D and the three operating pressures*
657 *(200, 300 and 400 kPa).*

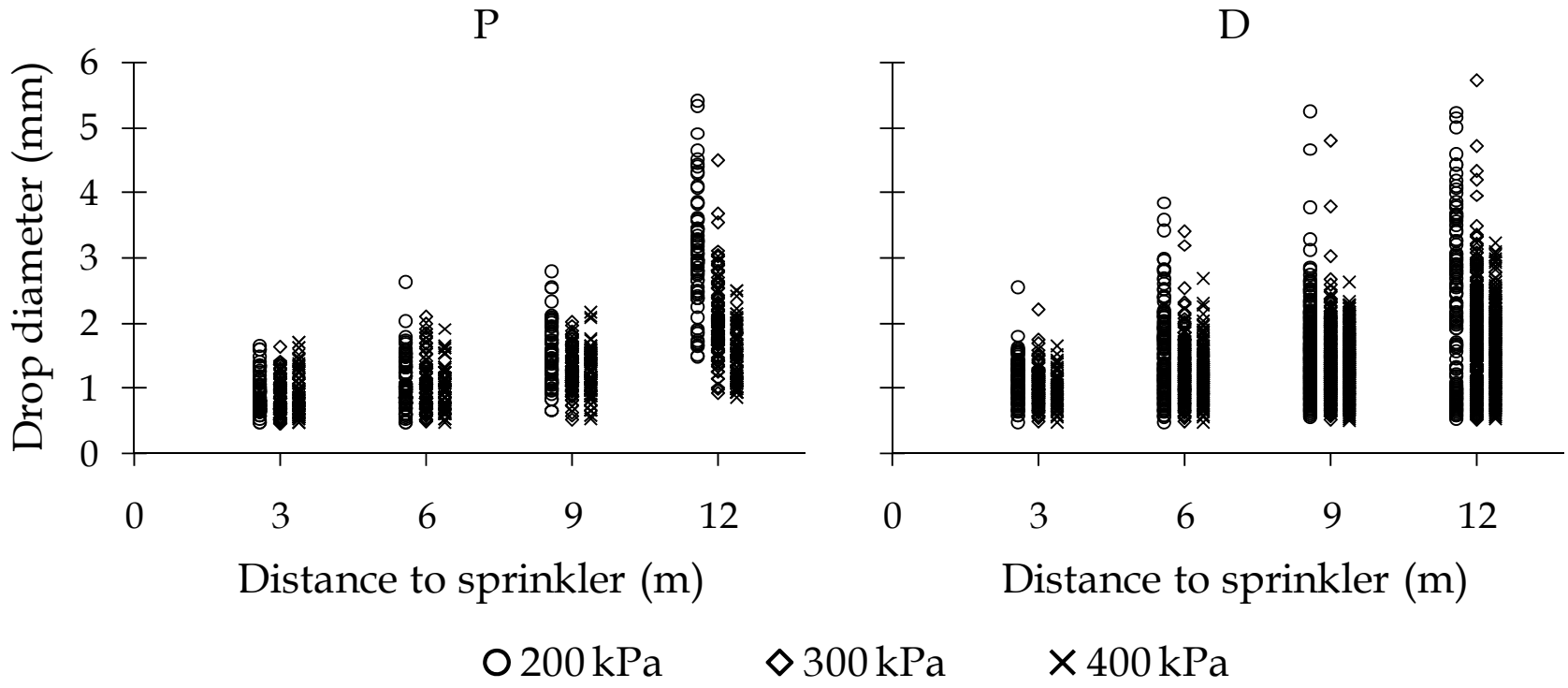

658

659

660 **Figure 5.** *Histographs of drop diameter for the P and D drop characterization methods and the three operating pressures.*

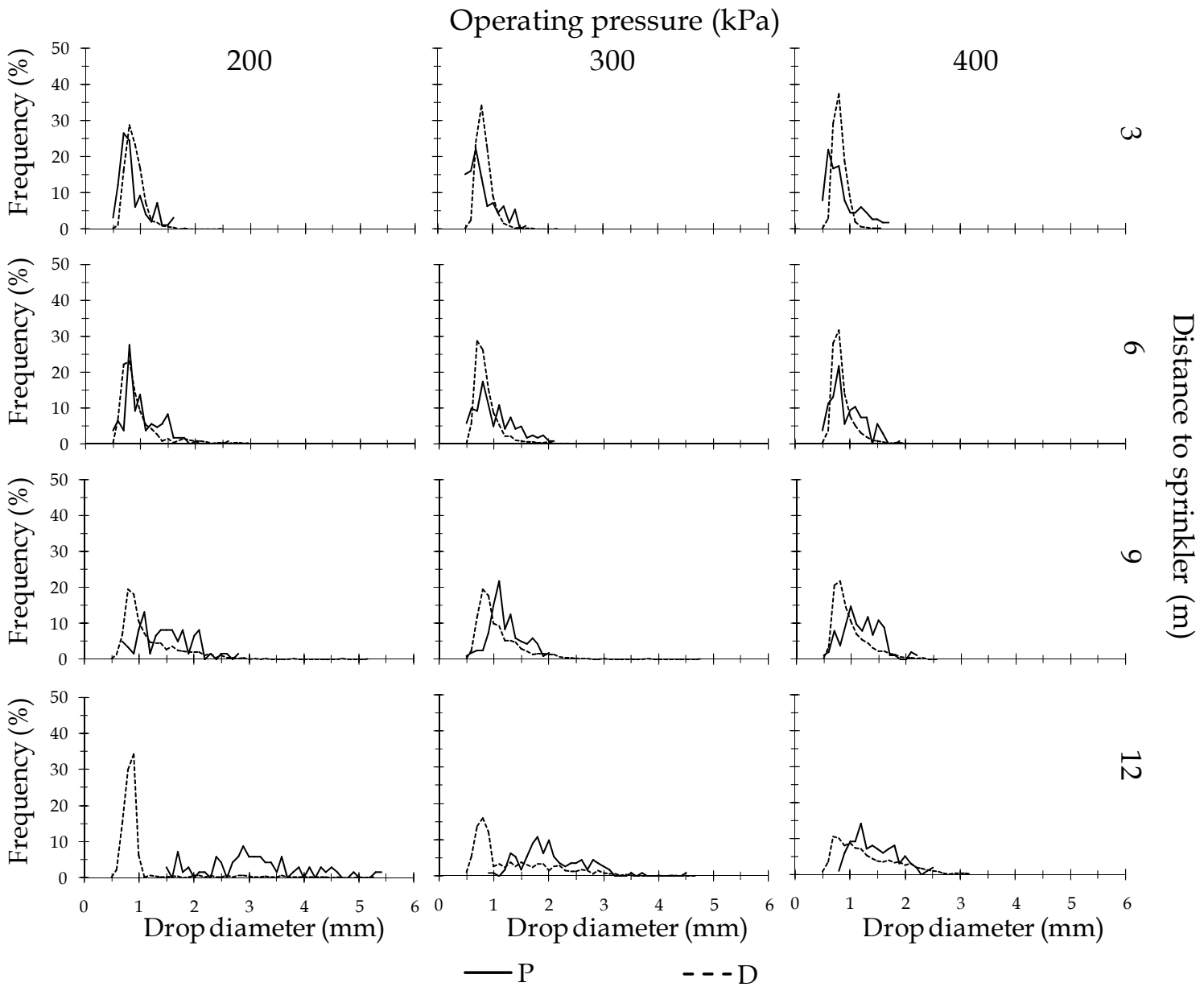

661

662 **Figure 6.** *Curves of cumulative drop frequency at 3, 6, 9 and 12 m from the sprinkler for the P and D drop characterization methods and the three operating*
663 *pressures.*

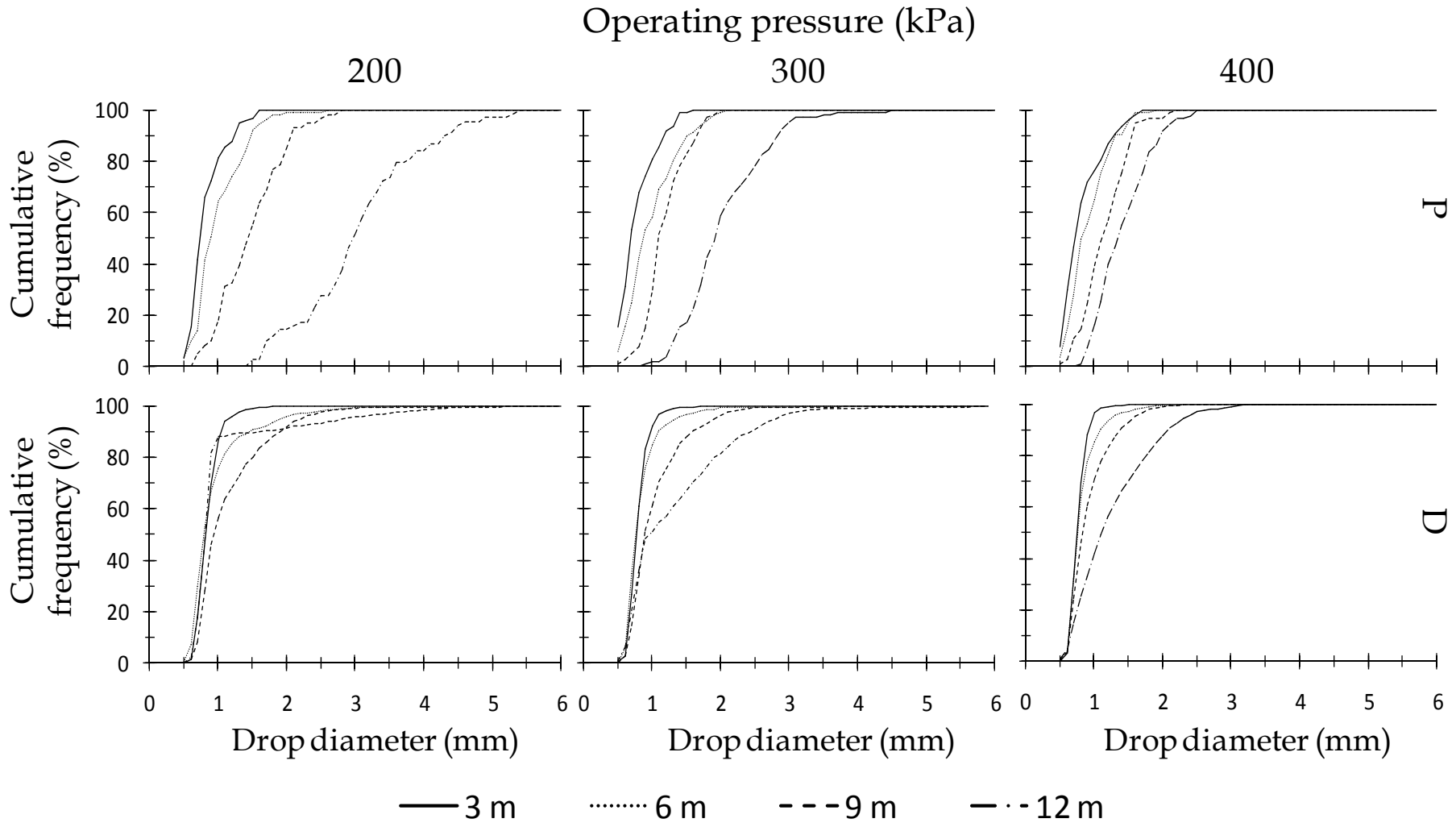

664

665

666 **Figure 7.** *Curves of cumulative application volume at 3, 6, 9 and 12 m from the sprinkler for the P and D drop characterization methods and the three operating*
667 *pressures.*

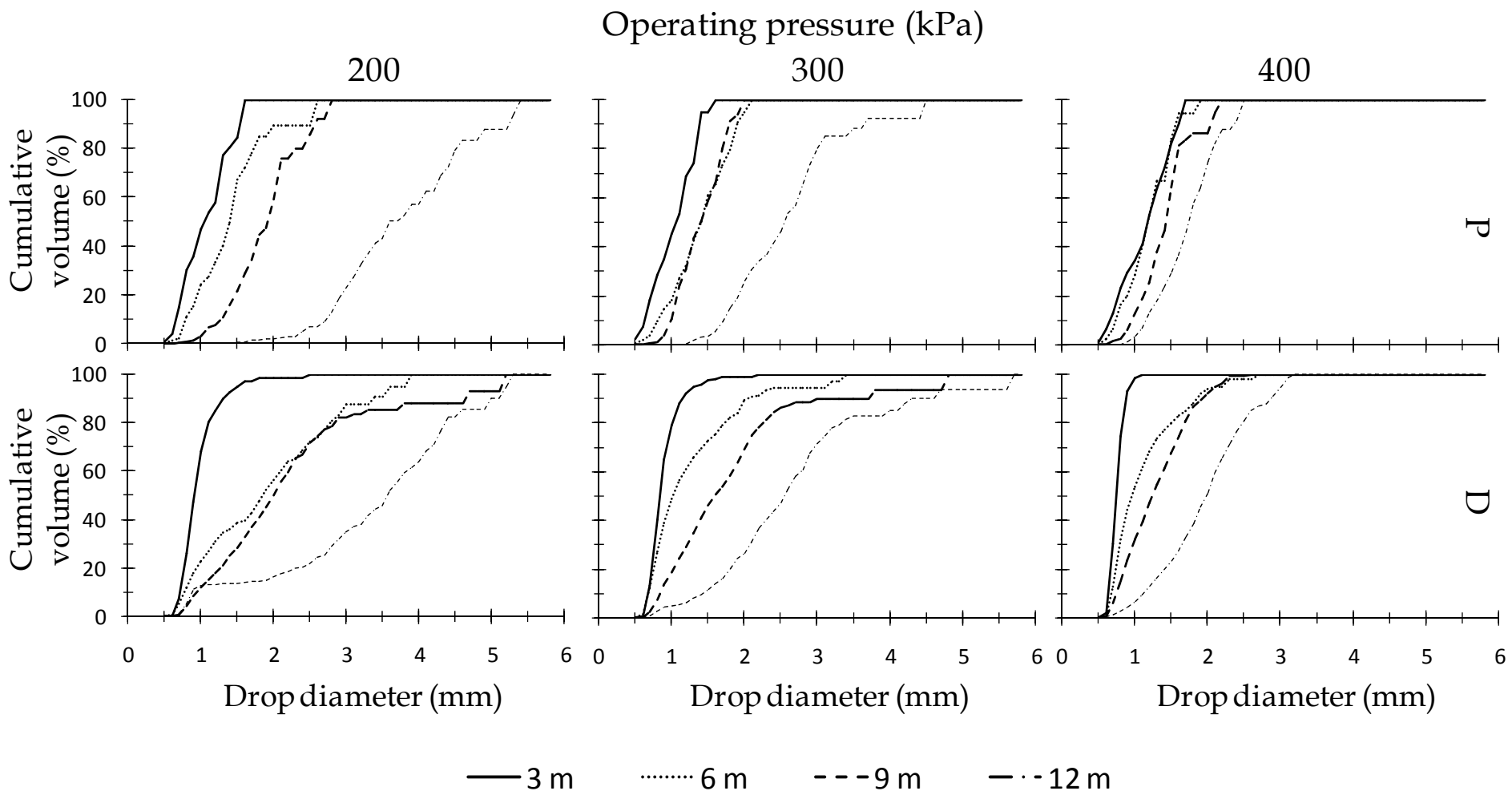

668

669

Figure 8. *Relationship between drop diameter and drop velocity for the photographic method (P), the four distances to the sprinkler and the three operating pressures.*

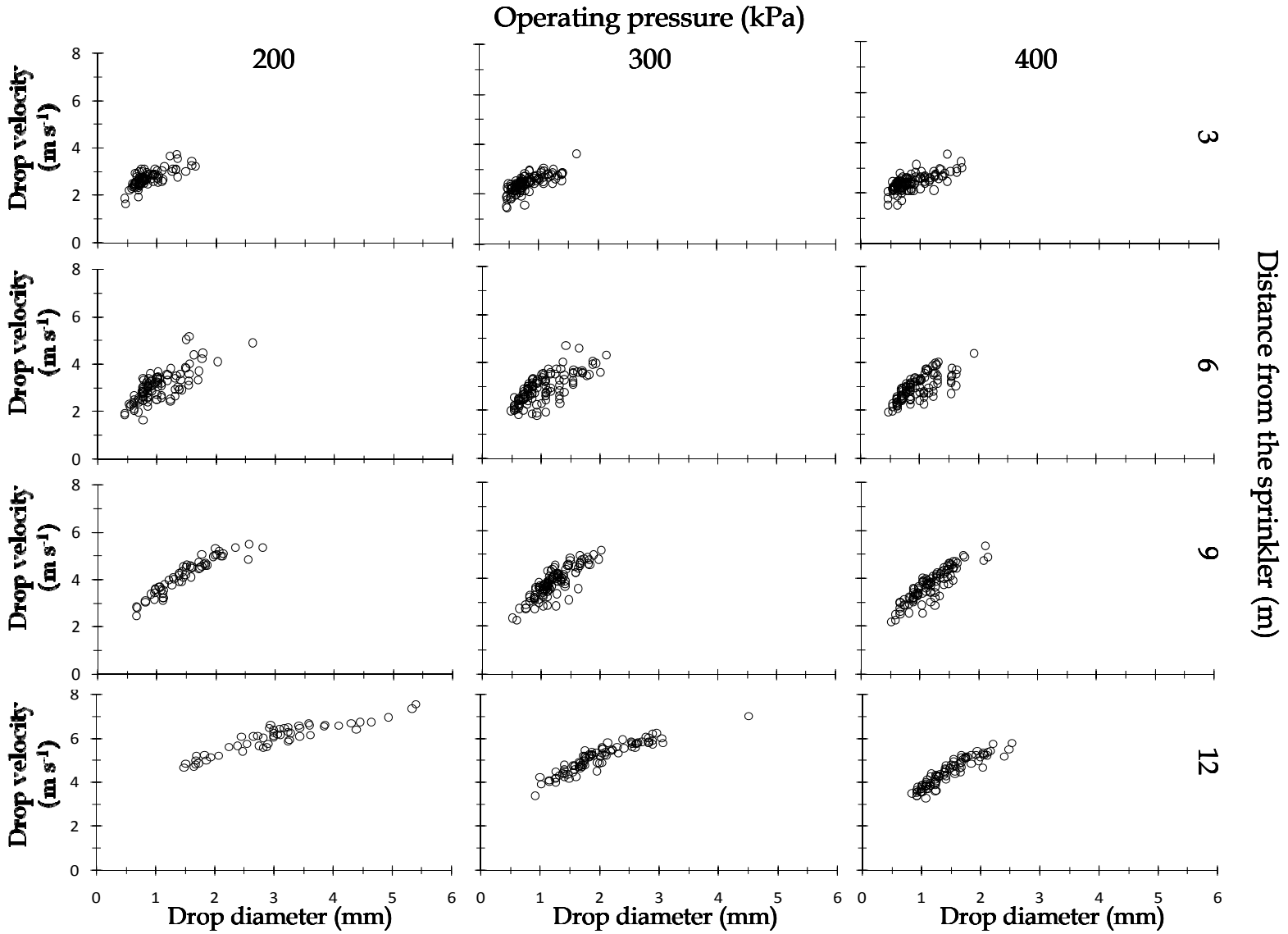

673 **Figure 9.** *Relationship between drop diameter and drop velocity obtained with the photographic method (P). Data are presented corresponding to the results of*
674 *Salvador et al. (2009) (using a pressure of 200 kPa and different distances to the sprinkler) and to all the experimental results reported in this paper (using*
675 *different pressures and distances to the sprinkler). The logarithmic regression, coefficient of determination (R^2) and standard error (SE) were obtained pooling both*
676 *data series.*

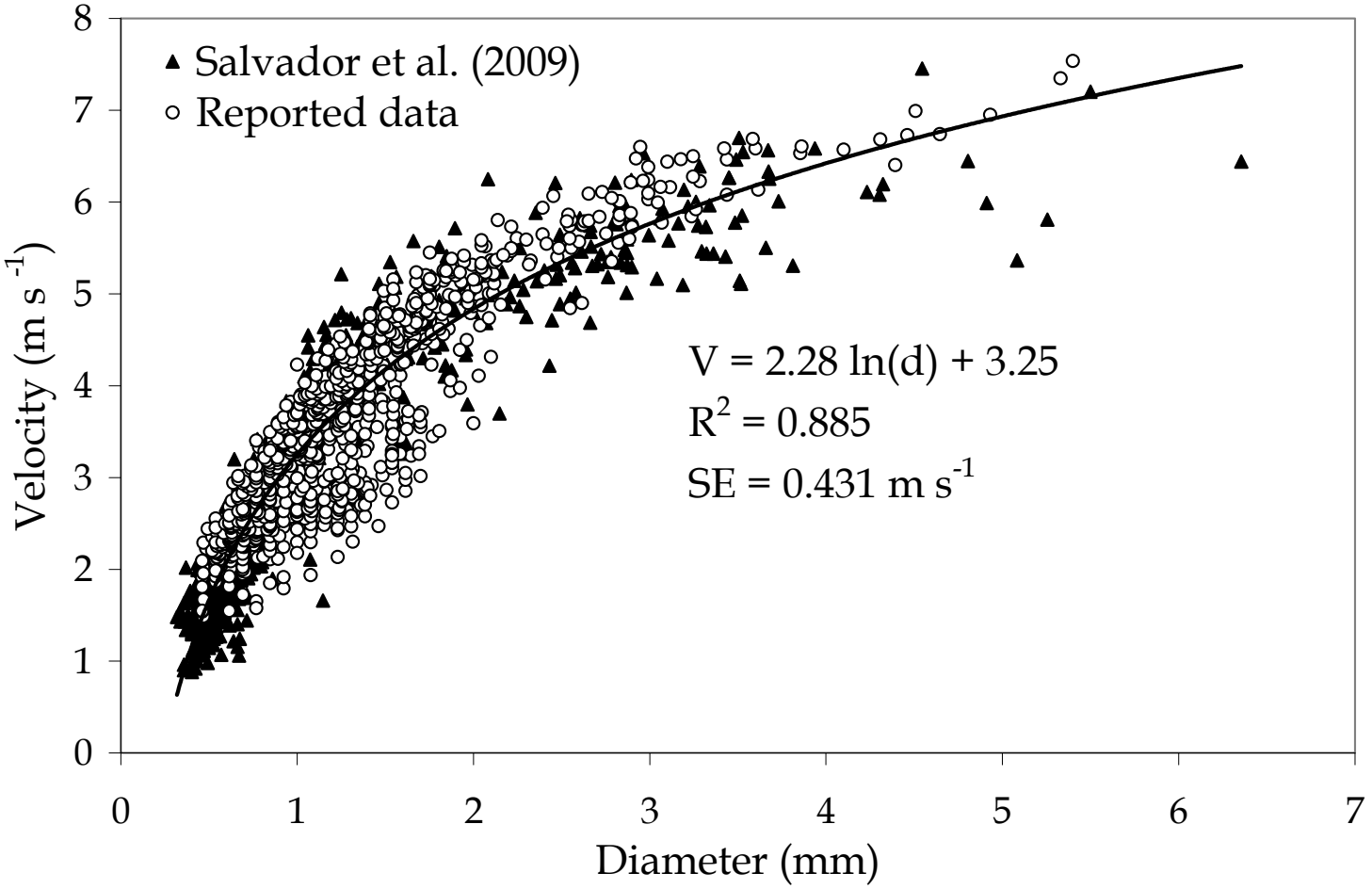

677

678

679 **Figure 10.** *Relationship between drop diameter and drop angle for the photographic method (P). Results are presented for the four observation distances and the*
680 *three operating pressures. The dashed line represents an angle of 90° (vertical drop trajectory).*

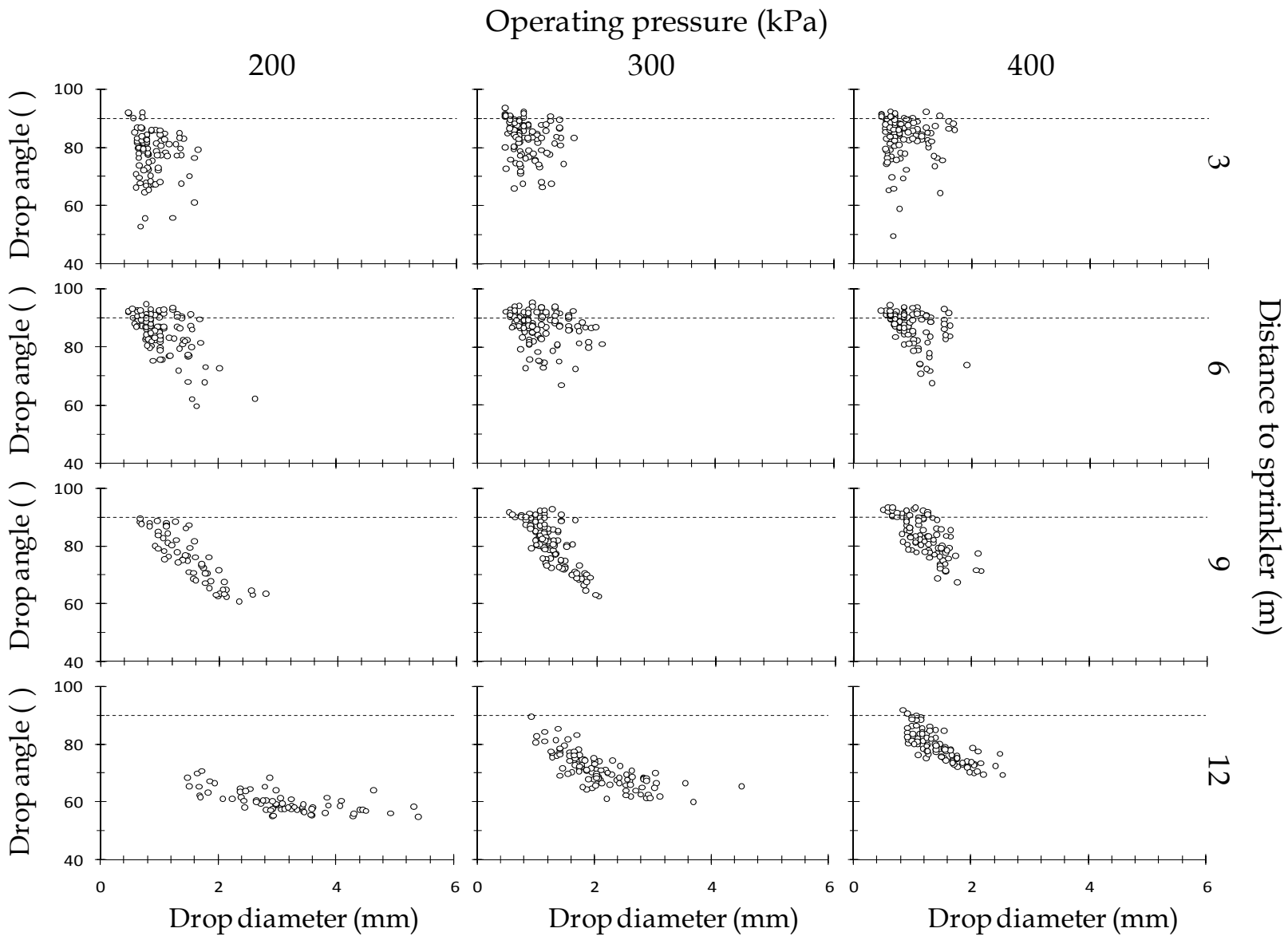

681